A Nighttime Visibility Meter for Secondary Roads

Eric Dumont[1], Roland Brémond[1],
Hicham Choukour[1], Yannick Guillard[2]

(1) Laboratoire Central des Ponts et Chaussées, Paris, France

(2) Laboratoire Régional des Ponts et Chaussées de Strasbourg, France

VIZIR project (MEEDDAT #05MT6039)
Headlight Visibility and Glare project (CalFrance #3530)

April 7, 2009

Contents

Introduction

It is the job of highway managers to sustainably ensure the mobility and safety of road users at all times. On rural highways at night, drivers can only rely on their vehicle headlamps to detect potential hazards on the roadway in time to take evasive actions. The visibility of an object ahead is directly related to the contrast between the object and its background, in this case the pavement. Consequently, it depends on the road surface reflective properties. In this report, we present a highway visibility meter tool to measure the impact of the pavement on nighttime visibility distance along the road. The system we propose is intended for highway managers to rate the visibility they offer to drivers at night, to locate road sections where nighttime visibility is poor, and to prioritize countermeasures.

Our approach to rate nighttime visibility is inspired by lighting system design practice. Street lamps and headlamps share the same purpose, which is to allow drivers to see traffic control devices (the markings for guidance and the signs for direction) and obstacles at night. The difference lies in the fact that a roadside lighting installation can (and should) be optimized by taking into account the photometric properties of the particular pavement it is meant to illuminate, whereas vehicle front-lighting systems will meet all kinds of road surfaces along various highways. Hence, the influence of road surface photometric characteristics on the visibility of objects under headlight illumination has rarely been studied, contrary to road lighting.

The first chapter presents our nighttime visibility metering approach, based on a conventional nighttime driving scenario, a computational target visibility model and a retroreflectivity monitoring apparatus. The implementation of this approach is detailed in the second chapter, with a special section on headlight glare. The third chapter gives sample results showing that darker pavement materials seem to serve best the visibility under headlight illumination, and that the proposed nighttime visibility meter can indeed be used to locate pavement sections where an obstacle may surprise the drivers.

Chapter 1

Concept

1.1 A conventional scenario

It is standard practice for the designers of both automotive and road equipment to rely on conventional driving scenarios to assess the performance of their designs. In the case of lighting systems, these scenarios mostly involve small obstacles or pedestrians which must be detected by the driver in time to avoid a collision [1, 6, 10, 24]. In the present work, we chose to focus on small obstacles for two reasons: because the visibility of pedestrians is a more complex problem in which we feel the pavement reflective properties are less relevant, and because conclusions pertaining to a small target will apply to pedestrians, only with less significance. The following parameters are summarized in Table 1.1, and the geometry is described in Figure 1.1.

The original scenario is that of a passenger car on a rural road without traffic, illuminating the roadway with high-beam headlamps (supposedly [21]). Except for the retro-reflected luminance coefficient of the pavement, the values of all geometric and photometric parameters are set to "standard" values found in the literature.

The eyes of the driver are 1.2 m above the ground and the headlamps mounting height is 0.65 m [14]. These values were set by European countries participating in the COST331 action on road marking visibility. They are slightly different from those reported by an SAE task force on headlamp mounting height in 1996 [11], with no significant effect.

The headlighting beam pattern is the median (50th-percentile) European high-beam pattern as measured by UMTRI in 2001 [16]. UMTRI has published more recent data, but it only concerns the US market, and there is no comparable initiative in Europe that we are aware of. We discarded the constant intensity beam pattern defined in the framework of the COST331 action [14] as an over-simplified

alternative.

The obstacle is a square object of 0.18 m side [9] with a luminance factor of 8% [6], standing in the middle of the lane. The choice of a small dark target is based on common practice in headlight visibility studies [10, 27]. We initially considered darker targets, with luminance factor values as low as 6% (to have a contrast close to 30%, similarly to a 20% target under street lighting [9], only in positive contrast) or even 4% (as measured from tire treads, which constitute a credible candidate for a small obstacle on the road), but they led to extremely small visibility distances.

The road is a 7 m wide 2-lane highway. The retroreflected luminance coefficient of the pavement is measured along the road with the ECODYN (mlpc®) system described in Section 1.3, and determines the visibility range of the small target.

Table 1.1: Nighttime visibility parameters, and their values in the conventional scenario.

	Parameter	Value	Description
Headlamps	s	1 m	Distance between headlamps
	h	0.65 m	Mounting height
Driver	A	25 y	Age
	d_{D}	1.8 m	Distance behind the headlamps
	h_{D}	1.2 m	Eye height
Target	a	0.18 m	Size
	ρ	8%	Luminance factor
Road	w	7 m	Width

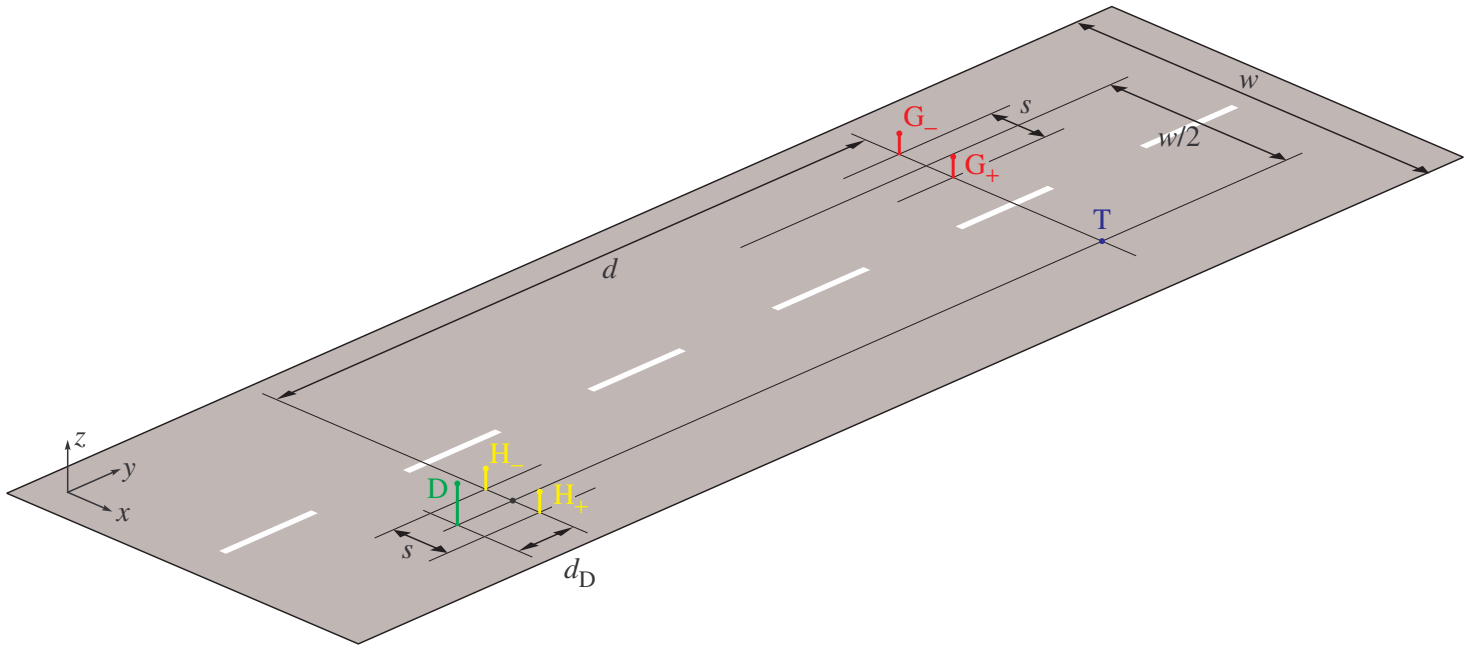

Figure 1.1: Geometry of the conventional scenario for assessing nighttime visibility. D: driver; T: target; $H_{\pm}$: left- and right-side headlamps; $G_{\pm}$: left- and right-side headlamps of oncoming traffic.

1.2 A computational model

For a given driver, with a given acuity and a given contrast sensitivity, the ability to detect a given achromatic object in a given traffic situation mainly depends on three parameters: object luminance, background luminance and adaptation luminance. To put it simply, the luminance difference required to detect an object on its background increases with the overall light level to which the driver is adapted.

The luminance difference threshold (i.e. the minimal detectable luminance difference) was investigated in laboratory conditions by Blackwell in the 1940's, with uniform discs on uniform backgrounds [2]. The results of his experiments, based on an extensive number of individual observations, now constitute a reference. He later proposed to use the ratio between actual contrast and threshold contrast as a visibility descriptor, and this so-called Visibility Level (VL) was adopted by the CIE to evaluate lighting design in terms of visual performance [3]:

$$V = \frac{C}{C_{\mathrm{th}}} = \frac{(L - L_{\mathrm{b}})/L_{\mathrm{b}}}{(L_{\mathrm{th}} - L_{\mathrm{b}})/L_{\mathrm{b}}} = \frac{\Delta L}{\Delta L_{\mathrm{th}}} \tag{1.1}$$

where C is the actual contrast and C_{th} the threshold contrast, L is the actual object luminance and L_{th} the object luminance at threshold contrast, L_{b} is the background luminance, ΔL is the actual luminance difference and ΔL_{th} the threshold luminance difference.

Given all the parameters, the most accurate way to calculate the threshold contrast, or threshold luminance difference, for a particular situation is to interpolate from Blackwell's laboratory data [19]. However, a more convenient method is to use analytic functions fitted to the laboratory data. Several such empirical models have been introduced in the past [13]. One of the most popular among lighting practitionners was proposed by Adrian in the 1980's for small targets (subtending less than 60 minutes of arc) [9]. Adrian's computational model is described in Appendix C.

1.3 A metering tool

ECODYN (mlpc®) is an apparatus developed by LCPC for monitoring the performance of road markings. Travelling at up to 110 km/h, it allows in-traffic measurements, as illustrated in the pictures of Figure 1.3. The device consists of a removable measurement box installed on the side of the vehicle. It contains a source of white light, emission-reception optics with mechanical modulation, and all electronic signal detection and processing circuits. The retroreflected luminance coefficient of the pavement and the marking is transmitted to an on-board

computer which synchronizes the acquisition with the relative position of the vehicle along the road, measured with an odometer, in order to make a record every 40 cm.

Figure 1.2: ECODYN (mlpc$^{(R)}$) was developed to monitor the performance of road markings, but it also measures the retroreflectivity of the pavement.

The geometry of the measurement follows the European standard EN 1436 on road marking performance for road users: 1.24° illumination angle and 2.29° observation angle, which roughly corresponds to a position 30 m ahead of the vehicle. This normally means that we can only use ECODYN measurements for assessing pavement luminance at 30 m, but previous studies on pavement retroreflectivity tend to show that the retroreflected luminance coefficient of pavement materials under headlamp illumination is relatively constant beyond this distance [7, 14]. Typical values are reported in Appendix A.

Chapter 2

Implementation

2.1 Filtering RL values

The ECODYN system can be fitted on both sides of the monitoring vehicle, and thus provide data about the pavement retroreflectivity on the left- and right-hand sides of the road. Sample data is presented in Figure 2.1. It can be seen that the measurements can be quite noisy. For road marking monitoring, the results are usually integrated on 150-m sections for easier interpretation by the road operator. We apply the same kind of pre-processing, only on a shorter basis arbitrarily set to 50 m. This length was chosen as a compromise between legibility and accuracy: 50 m corresponds to the safety distance at 90 km/h, so we felt it was a maximum. Practically, the pavement R_{L} at any position along the road is the average of the median of the left- and right-hand measured values on a 50-m length around that position.

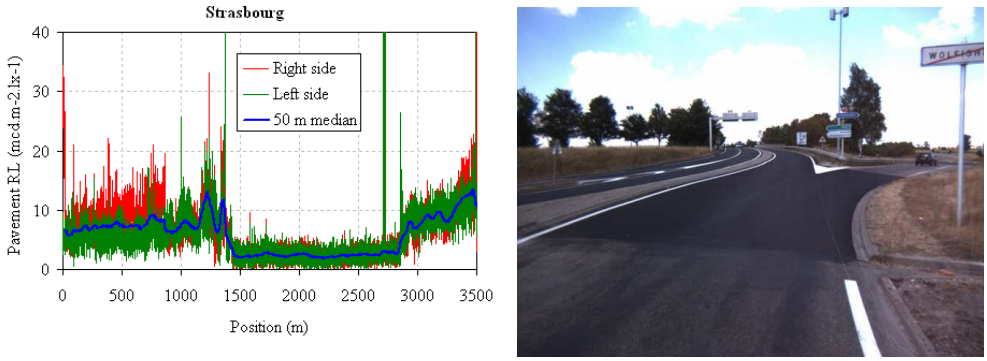

Figure 2.1: ECODYN measurements along a 3.5-km road section with asphaltic pavement (near Strasbourg, France).

The example in Figure 2.1 is interesting because it shows a section, between

about 1.5 and 3 km, with a different retroreflectivity profile. The pavement is more recent on that particular section, as can be seen in the picture taken at that spot. Fresh asphalt concrete is darker than weathered asphalt concrete, which explains the lower and more uniform retroreflectivity.

2.2 Setting VL parameters

There are several parameters that we need to compute in order to compute the VL of the considered target at a specified distance: target angular size, target luminance difference and adaptation luminance. We also need to set the observation time and the probability of detection.

2.2.1 Target size

The angular size α of the target depends on the distance from the driver. In Adrian's model, it must be expressed in arc minutes.

$$\tan\left(\frac{\pi}{180}\frac{\alpha/2}{60}\right) \approx \frac{a/2}{d_{\mathrm{D}}+d} \tag{2.1}$$

2.2.2 Target luminance

The luminance of the target L results from the illuminance generated by the headlamps and the luminance factor of the target. The illuminance in turn results from the intensity in the direction of the target. The illumination of the target by the headlamps is approximately perpendicular.

$$\begin{aligned} L &= \frac{\rho}{\pi}\left(E_{\mathrm{H}_-}+E_{\mathrm{H}_+}\right) \\ &\simeq \frac{\rho}{\pi}\left(E_{\perp\mathrm{H}_-}+E_{\perp\mathrm{H}_+}\right) \end{aligned} \tag{2.2}$$

with

$$\begin{aligned} E_{\perp\mathrm{H}_\pm} &= \frac{I_{\mathrm{H}_\pm}}{\mathrm{H}_\pm \mathrm{T}^2} \\ &= \frac{I_{\mathrm{H}_-}+I_{\mathrm{H}_+}}{(s/2)^2+d^2+h^2} \end{aligned} \tag{2.3}$$

hence,

$$L \simeq \frac{\rho}{\pi}\frac{I_{\mathrm{H}_-}+I_{\mathrm{H}_+}}{(s/2)^2+d^2+h^2} \tag{2.4}$$

where $I_{\mathrm{H}_\pm}$ are the intensities of the left- and right-hand side headlamps. These intensities are bilinearly interpolated from the tabulated beam pattern after computing the vertical and horizontal angles between the target direction and the headlamp axis, as illustrated for a single headlamp in Figure 2.2.

$$\tan\theta_{\mathrm{vH}_\pm} = \frac{z_\mathrm{T} - z_{\mathrm{H}_\pm}}{y_\mathrm{T} - y_{\mathrm{H}_\pm}} = -\frac{h}{d} \tag{2.5a}$$

$$\tan\theta_{\mathrm{hH}_\pm} = \frac{x_\mathrm{T} - x_{\mathrm{H}_\pm}}{\sqrt{(y_\mathrm{T} - y_{\mathrm{H}_\pm})^2 + (z_\mathrm{T} - z_{\mathrm{H}_\pm})^2}} = \frac{\pm s/2}{\sqrt{d^2 + h^2}} \tag{2.5b}$$

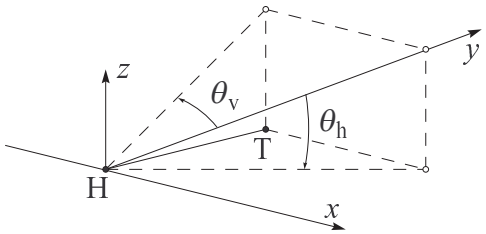

Figure 2.2: Illumination angles needed to extract the intensity emitted by a headlamp at H toward the target at T from the headlamp beam pattern.

2.2.3 Background luminance

How to set the background luminance to use Adrian's model with a non uniform background remains an unanswered question. Practically, it is usually dealt with in two ways: either the background luminance is set to the average luminance inside a "small" region around the target [27], or it is set to the luminance of the pavement at one of the borders of the target [10, 25]. Blackwell and Bixel tend to validate the second approach, stating that the visibility of targets in target-background complexes of non-uniform luminance can probably be best understood in terms of the contrast made by the target with respect to its background at the target border, and that it is not meaningful to describe target contrast in terms of the average luminance of the background [4]. We made the same somewhat arbitrary choice as Farber and Bhise, setting the background luminance to the luminance of the pavement at the base of the target [6]. Assuming that the target and the pavement at its base receive the same amount of illumination, and knowing the retroreflected luminance coefficient R_L of the pavement, we draw the following expression for the background luminance:

$$L_\mathrm{b} = R_\mathrm{L}\left(E_{\perp\mathrm{H}_-} + E_{\perp\mathrm{H}_+}\right) \tag{2.6}$$

hence, with (2.3),

$$L_{\mathrm{b}} = R_{\mathrm{L}} \frac{I_{\mathrm{H}_-} + I_{\mathrm{H}_+}}{(s/2)^2 + d^2 + h^2} \tag{2.7}$$

The resulting expression for the luminance difference between the target and its background is:

$$\Delta L = \left(\frac{\rho}{\pi} - R_{\mathrm{L}} \right) \frac{I_{\mathrm{H}_-} + I_{\mathrm{H}_+}}{(s/2)^2 + d^2 + h^2} \tag{2.8}$$

An interesting outcome of our choice for setting the background luminance is that the contrast of the target is independent of headlamps illumination.

$$C = \frac{\Delta L}{L_{\mathrm{b}}} = \frac{\rho}{\pi R_{\mathrm{L}}} - 1 \tag{2.9}$$

2.2.4 Adaptation luminance

The question which remains to be settled in order to compute the VL is whether the driver is adapted to the background luminance L_{b}, or if the adaptation luminance L_{a} should be used instead as proposed by Adrian [9]. Practically, the adaptation luminance in headlight illumination conditions is generally unknown [26], although a couple of experimental methods have been proposed to estimate it [10, 12]. In headlight visibility studies, the adaptation luminance is usually set to the background luminance, although it is sometimes set to the average luminance around the object or over some region at the center of the driver's field of view [25, 28]. We use the typical assumption that $L_{\mathrm{a}} = L_{\mathrm{b}}$.

2.2.5 Correction factors

Like most VL-based visibility studies, we chose to set the target exposure time to 200 ms, which is based on observations of eye movements while driving [5, 8]. As for the probability of detection, we chose to use the same value as the one introduced by Adrian in his model [9]: $F_{\mathrm{p}} = 2.6$, which corresponds to a probability of 99.96% according to C.4. The age of the driver, which also affects the threshold, was set to 25 y in the conventional scenario.

2.2.6 Numerical application

As an example, let us consider the case where the small target is set 60 m ahead of the vehicle, with typical values reported by the COST331 Action for the pavement retroreflectivity ($R_{\mathrm{L}} = 15\,\mathrm{mcd.m^{-2}.lx^{-1}}$) and the headlamps intensity ($I_{\mathrm{H}\pm} = 10\,\mathrm{kcd}$). In that case, the target luminance is $L = 0.141\,\mathrm{cd.m^{-2}}$, the pavement

luminance is $L_{\mathrm{p}} = 0.083\,\mathrm{cd.m^{-2}}$. The resulting contrast is $C = 69.8\%$. According to Adrian's model, the threshold luminance difference in these conditions is $\Delta L_{\mathrm{th}} = 0.022\,\mathrm{cd.m^{-2}}$, which sets the VL of the target to 2.65.

2.3 Visibility distance from VL

2.3.1 Field factor

Theoretically, an object with VL $= 1$ is just noticeable. However, threshold contrasts measured in operational conditions are always higher than the threshold contrasts predicted from laboratory data because of the driving task demand [5, 20, 23]. This is dealt with by a so-called field factor, which can also be interpreted as a threshold VL for visibility in actual traffic situations as opposed to laboratory conditions. With a theoretical analysis on how to set a value for the field factor, Dunipace et al suggest that VL $= 15$ should be an adequate visual requirement for highway driving with a detection probability of 99% ($F_{\mathrm{p}} = 2$) [5]. They also argue that the field factor is smaller in the case of road tests, mostly because of the controlled test procedures. The experimental analysis by Ising et al gives compatible conclusions, with required visibility levels of 1 to 23 for alerted drivers [20]. These field factor values corroborate those proposed for roadway lighting by Adrian [8]: 15 to 20 for night-time driving, with 6 or 7 as a strict minimum for safety, considering a detection probability over 99.9% ($F_{\mathrm{p}} = 2.6$). IESNA recommends VL values between 2.6 and 3.8 (depending on road category) for an even higher detection probability ($F_{\mathrm{p}} = 2.9$) [15]. We chose to adopt Adrian's VL threshold value of 7 in order to be consistent with the French recommendations on roadway lighting [17].

2.3.2 Visibility distance

Computing the distance at which the VL of the target equals a specified value cannot be done analytically with Adrian's model. The solution, inspired by the COST331 Action [14], is to iteratively set the headlamps closer and closer to the target until the previously chosen threshold VL is reached. This gives us the visibility distance, which we can confront to the "safe distance", i.e. the distance covered at legal speed during the 2 s time usually considered as the minimum time needed for an evasive action. It should be noted that as the distance gets smaller, the target contrast remains constant (as predicted by (2.9)) while its angular size and background luminance both increase, resulting in a lower ΔL_{th}, and thus in a higher VL and a higher visibility distance. This is clearly illustrated in the

graph of Figure 2.3, which was obtained for a pavement retroreflected luminance coefficient of 15 mcd.m^{-2}.lx^{-1}.

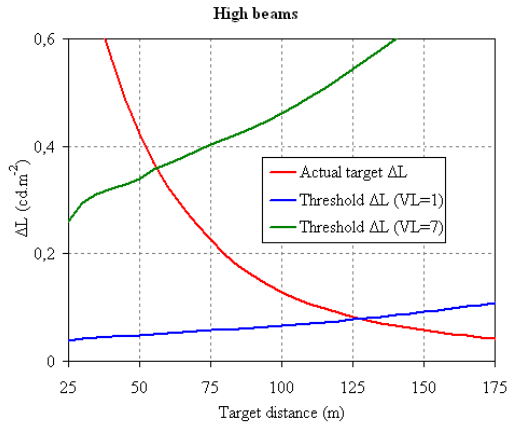

Figure 2.3: Target luminance difference and threshold luminance difference as a function of target distance in the high-beam situation. The target luminance factor is 8%, and the pavement retroreflected luminance coefficient is 15 mcd.m^{-2}.lx^{-1}. A field factor of 7 yields a visibility distance of 56 m.

2.4 Introducing headlight glare

In the conventional scenario presented in Section 1.1, the headlamps are set on high beam because the driver is alone on a highway without roadway lighting. But with ever increasing traffic, there is a chance that the driver will meet oncoming vehicles. A potential obstacle on the roadway will be all the more difficult to detect, for two reasons: the driver must switch to low beam, and he will suffer glare from the headlamps of the oncoming vehicle. Headlamps produce two types of glare [22]: disability glare refers to an objective impairment in visual performance while discomfort glare refers to a subjective annoyance. In our study, we focus on disability glare because it can be accounted for in Adrian's model, and thus its impact on our nighttime visibility index can be assessed.

The masking effect of disability glare, caused by intraocular scatter, is comparable with the effect of an overimposed veiling luminance L_{eq} which depends on the illuminance E_{g} from the glare source at the eye and the angular distance θ between the glare source and the line of sight. The veiling luminance is also affected by the age A of the observer.

$$\frac{L_{\mathrm{eq}}}{E_{\mathrm{g}}} = \frac{10}{\theta^3} + \frac{5}{\theta^2}\left(1 + \left(\frac{A}{62.5}\right)^4\right) \tag{2.10}$$

The Small Angle Disability Glare Equation (2.10), adopted by the CIE in 2002, is valid in the restricted angular range $0.1^\circ < \theta < 30^\circ$, which leaves out the influence of ocular pigmentation at very small angles [18]. It describes glare from point light sources, and must be integrated over the angular aperture in case of extended light sources.

In order to introduce headlight glare into our conventional scenario, we needed to define the position of the oncoming vehicle, so we arbitrarily chose to set it so that its headlamps were at the same distance as the target, as illustrated in Figure 1.1. Assuming that the line of sight of the driver is set onto the target, the excentricity of the headlamps is obtained as follows:

$$\begin{aligned}\cos\theta_\pm &= \frac{\overrightarrow{\mathrm{DG}_\pm}.\overrightarrow{\mathrm{DT}}}{\mathrm{DG}_\pm\,\mathrm{DT}} \\ &= \frac{(d+d_\mathrm{D})^2+(h_\mathrm{D}-h)\,h_\mathrm{D}}{\sqrt{\left[\left(-\frac{w}{2}\pm\frac{s}{2}\right)^2+(d+d_\mathrm{D})^2+(h_\mathrm{D}-h)^2\right]\left[(d+d_\mathrm{D})^2+h_\mathrm{D}^2\right]}}\end{aligned} \tag{2.11}$$

and so the illuminance they produce at the eye of the driver is:

$$E_{\mathrm{G}_\pm} = \frac{I_{\mathrm{G}_\pm}\,\cos\theta_\pm}{{\mathrm{DG}_\pm}^2} \tag{2.12}$$

The intensities $I_{\mathrm{G}_\pm}$ are interpolated from the tabulated beam pattern, after computing the vertical and horizontal angles between the driver direction and the axis of the headlamps:

$$\tan\theta_{\mathrm{vG}_\pm} = \frac{z_\mathrm{D}-z_{\mathrm{G}_\pm}}{y_\mathrm{D}-y_{\mathrm{G}_\pm}} = \frac{h-h_\mathrm{D}}{d+d_\mathrm{D}} \tag{2.13a}$$

$$\begin{aligned}\tan\theta_{\mathrm{hG}_\pm} &= \frac{x_\mathrm{D}-x_{\mathrm{G}_\pm}}{\sqrt{(y_\mathrm{D}-y_{\mathrm{G}_\pm})^2+(z_\mathrm{D}-z_{\mathrm{G}_\pm})^2}} \\ &= \frac{-w/2\pm s/2}{\sqrt{(d_\mathrm{D}+d)^2+(h_{\mathrm{G}_\pm}-h)^2}}\end{aligned} \tag{2.13b}$$

The veiling luminance L_v produced by both headlamps is the sum of the glare luminance values computed for each headlamp with Equations (2.10), (2.11) and (2.12).

The total glare luminance L_v is added to both the target luminance and the background luminance, so the target contrast is lowered but the luminance difference ΔL remains unaffected. However, the glare luminance is also added to the adaptation luminance ($L_\mathrm{a} = L_\mathrm{b} + L_\mathrm{v}$), which results in a lower VL for the target. In effect, the visibility distance is reduced, as illustrated in Figure 2.4.

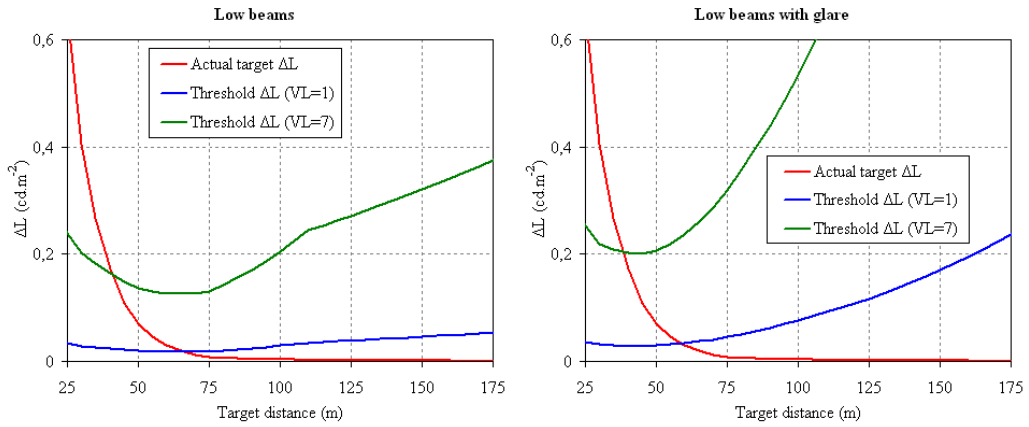

Figure 2.4: Target luminance difference and threshold luminance difference as a function of target distance in the low-beam situation, without and with headlight glare from oncoming traffic. The target luminance factor is 8%, and the pavement retroreflected luminance coefficient is 15 $mcd.m^{-2}.lx^{-1}$. A field factor of 7 yields a visibility distance of 41 m without glare, and 36 m with glare.

Chapter 3

Results

3.1 Target luminance factor vs. pavement retroreflectivity

When considering a target on the pavement ahead of the vehicle, illuminated by high-beam headlamps, we intuitively expect a positive contrast because the target is (almost) perpendicular to the lighting direction, while the pavement is illuminated at a grazing angle. This leads to the rather counter-intuitive deduction that the pavement needs to be as dark as possible for the target to be more visible. But it suffices to consider the expression of the contrast as a function of the target luminance factor and pavement retroreflected luminance coefficient to see that for dark enough targets, the contrast can be negative. In such cases, the pavement needs to be as light-colored as possible to maximize the visibility. On the other hand, the range of luminance factors which make the obstacle "invisible" is smaller with darker pavements. This can be clearly seen in Figure 3.1. More details are provided in Appendix D.

3.2 Tests on field data

The Public Works Laboratory of Strasbourg made ECODYN measurements on several road sections to test our nighttime visibility meter tool. The measured R_{L} profiles are presented in Figure 3.2. They give an idea of the variations in retroreflectivity that one can expect when driving along the highway. The nighttime visibility distance profiles computed with our approach are presented alongside the measurements. Unfortunately, the range of measured R_{L} values is limited: we only have asphalt concrete pavements, with a maximum around 8 mcd.m^{-2}.lx^{-1}.

The measurements presented in Section 2.1 are more interesting, because of

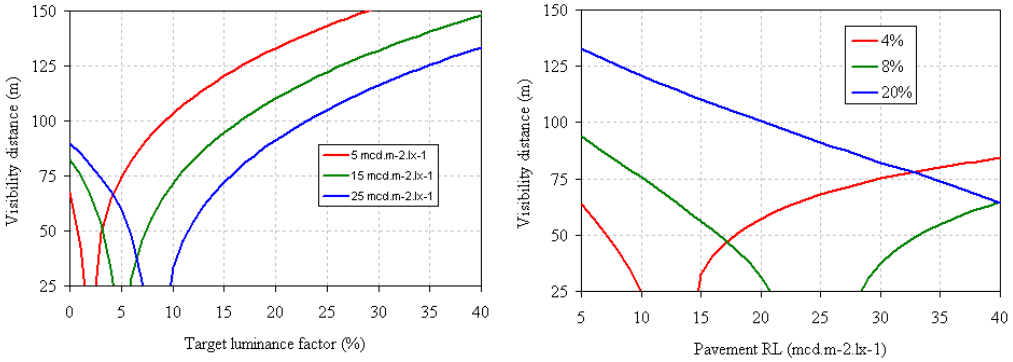

Figure 3.1: Visibility distance of 18-cm gray target under high-beam illumination in the middle of the road as a function of the luminance factor (left) and pavement retroreflected luminance coefficient (right).

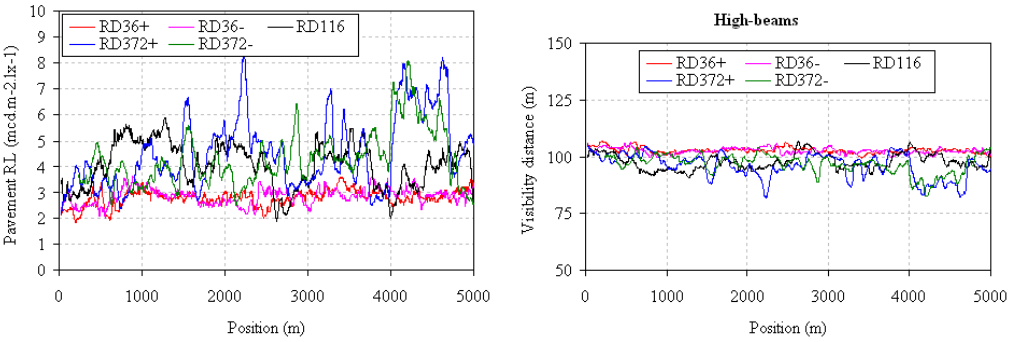

Figure 3.2: Median-filtered retroreflectivity profiles measured with ECODYN along several road sections (left), and computed nighttime visibility distance profiles for high-beam illumination (right).

the higher range of retroreflectivity (up to 13 mcd.m^{-2}.lx^{-1}) and because of the presence of a discontinuity. As expected, the first graph in Figure 3.3 shows that the darker section between 1.5 and 3 km provides a higher visibility, hence more reaction time, to the driver, with a 20% increase in visibility distance (from 85 m to 105 m). There are also local peaks of retroreflectivity (around 1.25 and 3.5 km) which bring the visibility distance down to 65 m. This is still acceptable as regards the 2-s safety distance. However, when the driver meets oncoming traffic and switches to low-beam, the visibility drops below the 50-m minimum. And should the driver stay in low-beam after crossing the other vehicle, the visibility is barely above the minimum even though the driver no longer suffers from disability glare. These findings concern a young driver, but the computational model we use allows us to investigate the influence of driver age. The second graph of Figure 3.3 shows that older drivers may be surprised by a dark obstacle on the light-colored pavement sections of the highway, with retroreflected luminance coefficient values above 10 mcd.m^{-2}.lx^{-1}.

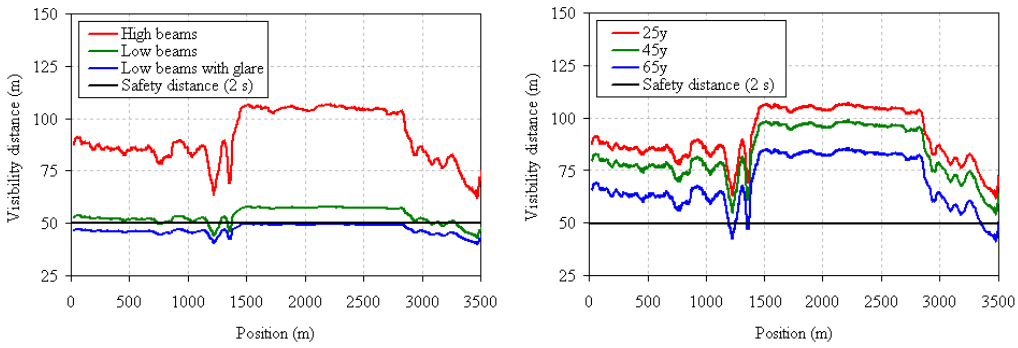

Figure 3.3: Computed nighttime visibility distance profiles along a 3.5 km road section, as a function of illumination conditions (left) and driver age (right).

Conclusion

We propose a nighttime visibility meter tool for secondary roads devoid of roadway lighting. The tool is based on a conventional driving scenario, a computational visibility model, and a retroreflectivity monitoring apparatus. It takes pavement retroreflected luminance coefficient profiles as input, and produces small target visibility distance profiles as output. Such profiles can serve to locate local discontinuities where an obstacle on the roadway might surprise the drivers at night under headlight illumination.

The preliminary tests performed with the proposed tool brought encouraging results. However, we need to address several questions before the nighttime visibility tool can be implemented for highway inspection. First, we need to assess the influence of the forward reflection of headlight on the pavement, which we have neglected so far. Second, we need to assess the correctness of using the pavement luminance at the base of the target as the background and adaptation luminance in the visibility model, and maybe consider a better definition of contrast. Last but not least, we need to validate the arbitrary choices on which we have built our tool, and to calibrate the output, and that will involve psychometric experiments. And after we have gone through these questions, we should consider taking the geometry of the road into account, because headlight illumination varies in bends and slopes.

Headlight glare was introduced into the conventional scenario, but disability glare alone has been considered so far, because it impairs visual performance with a direct impact on target visibility distance. However, discomfort glare is also affected by pavement retroreflectivity, as it takes a background luminance parameter[29]. The problem is we need to increase the background luminance to reduce discomfort glare. This calls for light-colored pavement materials, while we have seen that target visibility was best served by dark pavement materials. Hence, we should also consider discomfort glare in future work, as an additional index to evaluate the quality of service of the roadway in terms of nighttime visibility.

Acknowledgements

This work was funded by the Road Traffic and Safety Direction (DSCR) of the French Department of Transportation (MEEDDAT) in the framework of the VIZIR project (contract #05MT6039). Taking headlight glare into account was made possible by additional funding in the framework of the CalFrance partnership between California Department of Transportation (Caltrans) and MEEDDAT (contract #3530), which allowed fruitful knowledge sharing between the Visual Detection Lab of the University of California Berkeley and the Lighting and Visibility Team of LCPC.

The authors express their special thanks to Daniel Greenhouse and Kent Christianson, who provided many useful hints, and stayed out late at night on Richmond field to measure the visibility of the small target provided by Eric Dumont, or for net meetings with a 9-hour time difference between San Francisco and Paris. We also acknowledge the help of Laetitia Largenton (who did the measurements on the tire treads) and Stéphane Leboeuf (who came all the way to Guerville to make ECODYN measurements).

Bibliography

[1] Roper, V.J., Howard E.A. Seeing with Motor Car Headlamps. *Transactions of the Illuminating Engineering Society* **33**(5):417-438, 1938.

[2] Blackwell, H.R. Contrast Threshold of the Human Eye. *Journal of the Optical Society of America* **36**(11):624-643, 1946.

[3] A Unified Framework of Methods for Evaluating Visual Performance Aspects of Lighting. CIE Publication No. 19.2, 1972.

[4] Blackwell, H.R., Bixen, G.A. Visibility of Non-Uniform Target-Background Complexes. Ohio State University Research Foundation, 1963.

[5] Dunipace, D.W., Strong, J., Huizinga, M. Prediction of Nighttime Driving Visibility from Laboratory Data. *Applied Optics* **13**(11):2723-2734, 1974.

[6] Farber, E., Bhise, V. Development of a Headlight Evaluation Model. In *Driver Visual Needs in Night Driving*, TRB Special Report 156:23-39, 1975.

[7] Hubert, R., Canestrelli, M. Mesures de rétroréflexion sur chaussées sèches et mouillées. LCPC Report 1.20.0340.85, 1985.

[8] Adrian, W. Visibility Levels Under Night-time Driving Conditions. *Journal of the Illuminating Engineering Society* **16**(2):3-12, 1987.

[9] Adrian, W. Visibility of Targets: Model for Calculation. *Lighting Research and Technology* **21**(4):181-188, 1989.

[10] Olson, P.L. Aoki, T., Battle, D.S., Flannagan, M.J. Development of a Headlight System Performance Evaluation Tool. UMTRI-90-41, October 1990.

[11] Sivak, M., Flannagan, M.J. Partial Harmonization of International Standards for Low-Beam Headlighting Patterns. UMTRI-93-11, March 1993.

[12] Schnell, T. Development of a PC-based Pavement Marking Visibility Evaluation Model. Ohio University, 1994.

[13] Zwahlen, H.T., Schnell, T. Visual Target Detection Models for Civil Twilight and Night Driving Conditions. *Transportation Research Record* **1692**:49-65, 1999.

[14] Requirements for Horizontal Road Markings. COST331 final report, European Commission, 1999.

[15] American National Standard Practice for Roadway Lighting. ANSI/IESNA RP-8-00, 2000.

[16] Schoettle, B., Sivak, M., and Flannagan, M.J. High-Beam and Low-Beam Headlighting Patterns in the U.S. and Europe at the Turn of the Millennium. UMTRI-2001-19, May 2001.

[17] Recommandations relatives l'éclairage des voies publiques. Association Française de l'Éclairage, 2002.

[18] CIE Equations for Disability Glare. CIE Publication No. 146, 2002.

[19] Schnell, T., Aktan F. Enhanced Nighttime Visibility: Design and Implementation of TarVIP, a Visibility Prediction Model. University of Iowa, 2002 (draft).

[20] Ising, K.W., Fricker, T.R.C., Lawrence, J.M., Siegmund, G.P. Threshold Visibility Levels for the Adrian Visibility Model Under Nighttime Driving Conditions. SAE Technical Paper 2003-01-0294, 2003.

[21] Sullivan, J.M., Adachi, G., Mefford, M.L., Flannagan, M.J. High-Beam Headlamp Usage on Unlighted Rural Roadways. UMTRI-2003-2, February 2003.

[22] Vos, J.J. On the Cause of Disability Glare and its Dependence on Glare Angle, Age and Ocular Pigmentation. *Clinical and Experimental Optometry* **86**(6):363-370, 2003.

[23] Adrian, W., Stemprok, R. Required Visibility Levels in Road Scenes at Night Time Driving. In *Proc. ISAL 2005 (Darmstadt, Germany)*, pp.?-?, 2005.

[24] Blanco, M., Hankey, J.M., Dingus T.A. Enhanced Night Visibility Series: Phase II Study 1: Visual Performance During Nighttime Driving in Clear Weather. FHWA-HRT-04-134, December 2005.

[25] Gibbons, R.B., Hankey, J.M. Enhanced Night Visibility Series, Volume IX. U.S. Department of Transportation, 2005.

[26] Plainis, S., Murray, I.J., Charman, W.N. The Role of Retinal Adaptation in Night Driving. *Optometry and Vision Science* **82**(8):682-688, 2005.

[27] Kliebisch, D., Vlker, S. Measurement and Calculation of Detection Distances of Headlamp Light Distributions. In *Proc. ISAL 2007 (Darmstadt, Germany)*, pp., 2007.

[28] Visual Performance in the Mesopic Range. CIE TC1.58 Report, 2008 (draft).

[29] Christianson, K.B., Greenhouse, B.S., Barton, J.E., Chow, C. Methods to address headlight glare. California PATH TO#6603, 2009.

Appendix A

Pavement retroreflected luminance coefficient values

Hubert et al measured retroreflected luminance coefficient values between about 5 and 40 mcd.m^{-2}.lx^{-1} for typical pavement materials in dry condition [7]. The COST331 action reports values between 5 and 30 mcd.m^{-2}.lx^{-1} for asphaltic surfaces [14].

Table A.1: R_{L} values of typical pavement materials in dry condition [7].

Material		R_{L} (mcd.m^{-2}.lx^{-1})
Cement concrete		14
Surface dressing	(dark aggregate)	9-13
	(light-colored aggregate)	20-48
Asphalt concrete	(dark)	4-8
	(apparent aggregate)	9-15

Appendix B

Luminance factor of tire treads

In the conventional scenario presented in Section 1.1, the idea was to consider a potential small dark obstacle on the roadway. A tire tread was a credible candidate, so we measured the luminance factor of the used tire treads of several vehicles, as well as the luminance factor of a new tire tread, using a portable color-meter. The measured values are presented in Table B. We found luminance factor values around 3% for used tire treads, and close to 5% for an unused one.

Table B.1: Luminance factor ρ (and chrominance(x, y)) values measured on several tire treads with a color-meter, using CIE standard illuminant A.

Sample no.1 (75N7895E)				Sample no.2 (75N1956G)			
No.	ρ (%)	x	y	No.	ρ (%)	x	y
1	3.25	0.4518	0.4089	1	3.40	0.4443	0.4068
2	3.59	0.4494	0.4083	2	2.69	0.4463	0.4074
3	3.58	0.4500	0.4086	3	3.09	0.4451	0.4070
4	3.61	0.4491	0.4081	4	2.58	0.4464	0.4074
5	3.43	0.4500	0.4083	5	3.07	0.4467	0.4075
Sample no.3 (75N3715G)				Sample no.4 (new)			
No.	ρ (%)	x	y	No.	ρ (%)	x	y
1	3.38	0.4528	0.4092	1	4.78	0.4563	0.4104
2	3.52	0.4511	0.4085	2	4.85	0.4506	0.4091
3	3.07	0.4525	0.4084	3	4.80	0.4568	0.4105
4	3.21	0.4514	0.4085	4	4.68	0.4523	0.4097
5	3.54	0.4517	0.4086	5	4.95	0.4587	0.4106

Appendix C

Adrian's model for target visibility

C.1 Basic formula

$$\Delta L_{\mathrm{th}} = \left(\frac{\Phi^{\frac{1}{2}}}{\alpha} + L^{\frac{1}{2}} \right)^2 \tag{C.1}$$

where $\Phi^{\frac{1}{2}}$ and $L^{\frac{1}{2}}$ are defined in three ranges of the background luminance L_{b}.
If $L_{\mathrm{b}} \geq 0.6\,\mathrm{cd.m^{-2}}$:

$$\begin{aligned} \Phi^{\frac{1}{2}} &= \log\left(4.1925\, L_{\mathrm{b}}^{0.1556}\right) + 0.1684\, L_{\mathrm{b}}^{0.5867} \\ L^{\frac{1}{2}} &= 0.05946\, L_{\mathrm{b}}^{0.466} \end{aligned}$$

If $0.00418\,\mathrm{cd.m^{-2}} < L_{\mathrm{b}} < 0.6\,\mathrm{cd.m^{-2}}$:

$$\begin{aligned} \Phi^{\frac{1}{2}} &= -0.072 + 0.3372\, \log L_{\mathrm{b}} + 0.0866\, (\log L_{\mathrm{b}})^2 \\ L^{\frac{1}{2}} &= -1.256 + 0.319\, \log L_{\mathrm{b}} \end{aligned}$$

If $L_{\mathrm{b}} \leq 0.00418\,\mathrm{cd.m^{-2}}$:

$$\begin{aligned} \Phi^{\frac{1}{2}} &= 0.028 + 0.173\, \log L_{\mathrm{b}} \\ L^{\frac{1}{2}} &= -0.891 + 0.5275\, \log L_{\mathrm{b}} + 0.0227\, (\log L_{\mathrm{b}})^2 \end{aligned}$$

C.2 Correction factors

(C.1) only applies for long exposure times (2 s or more), positive contrast, young observers (in their 20's), and a 50% detection probability. But it can be extended to account for other sets of these important parameters by means of several multiplying factors for which Adrian also introduced analytic expressions.

C.2.1 Contrast polarity factor

The polarity factor F_{n} accounts for a negative contrast (target darker than the background).

$$F_{\mathrm{n}} = 1 - \frac{m\,\alpha^{-\beta}}{2.4\,\Delta L_{\mathrm{th}}} \tag{C.2}$$

where

$$\beta = 0.6\,L_{\mathrm{b}}^{-0.1488}$$

If $L_{\mathrm{b}} \geq 0.1\,\mathrm{cd.m^{-2}}$:

$$\log(-\log m) = -0.125\,\left(\log L_{\mathrm{b}} + 1\right)^2 - 0.0245$$

If $0.004\,\mathrm{cd.m^{-2}} < L_{\mathrm{b}} < 0.1\,\mathrm{cd.m^{-2}}$:

$$\log(-\log m) = -0.075\,\left(\log L_{\mathrm{b}} + 1\right)^2 - 0.0245$$

C.2.2 Time factor

The time factor Ft accounts for an exposure time e shorter than 2 s.

$$F_{\mathrm{t}} = 1 + \frac{a(\alpha, L_{\mathrm{b}})}{e} \tag{C.3}$$

where

$$a(\alpha, L_{\mathrm{b}}) = \frac{1}{2.1}\left(a(\alpha)^2 + a(L_{\mathrm{b}})^2\right)^{\frac{1}{2}}$$

with

$$\begin{aligned} a(\alpha) &= 0.36 - \frac{0.0972\,b(\alpha)^2}{b(\alpha)^2 - 2.513\,b(\alpha) + 2.7895} \\ b(\alpha) &= \log\alpha + 0.523 \end{aligned}$$

and

$$\begin{aligned} a(L_{\mathrm{b}}) &= 0.355 - \frac{0.1217\,b(L_{\mathrm{b}})^2}{b(L_{\mathrm{b}})^2 - 10.4\,b(L_{\mathrm{b}}) + 52.28} \\ b(L_{\mathrm{b}}) &= \log L_{\mathrm{b}} + 6 \end{aligned}$$

C.2.3 Age factor

The age factor F_{a} accounts for the age A of the observer. It is defined in two ranges.
If $23\,\mathrm{y} < A < 64\,\mathrm{y}$:

$$F_{\mathrm{a}} = \frac{(A - 19)^2}{2160} + 0.99$$

If $64\,\mathrm{y} < A < 75\mathrm{y}$:

$$F_{\mathrm{a}} = \frac{(A - 56.6)^2}{116.3} + 1.43$$

C.2.4 Probability factor

Finally, the probability factor F_{p} accounts for a probability of detection p higher than 50% [8].

$$F_{\mathrm{p}} = \left(\frac{\ln(1-p)}{\ln(0.5)}\right)^{\frac{1}{2.532}} \tag{C.4}$$

Appendix D

Target luminance factor vs. pavement retroreflectivity

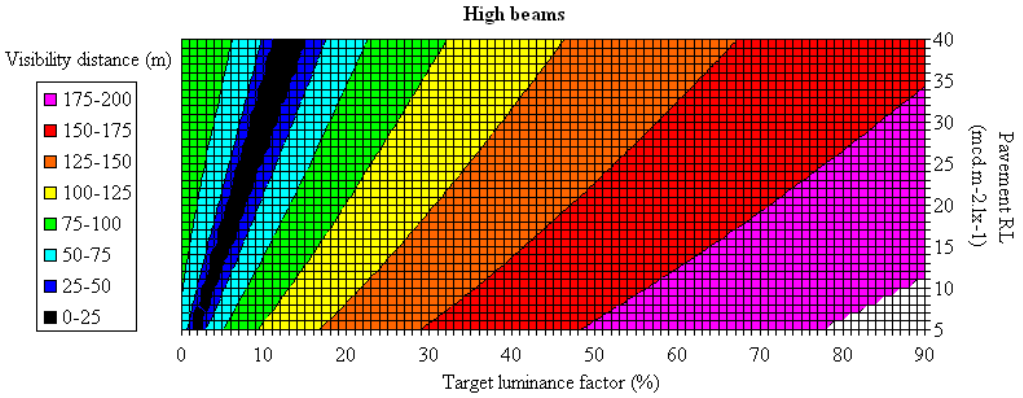

Figure D.1: Visibility distance of an 18-cm grey target in the middle of the road under high-beam illumination as a function of the target luminance factor and pavement retroreflected luminance coefficient

.

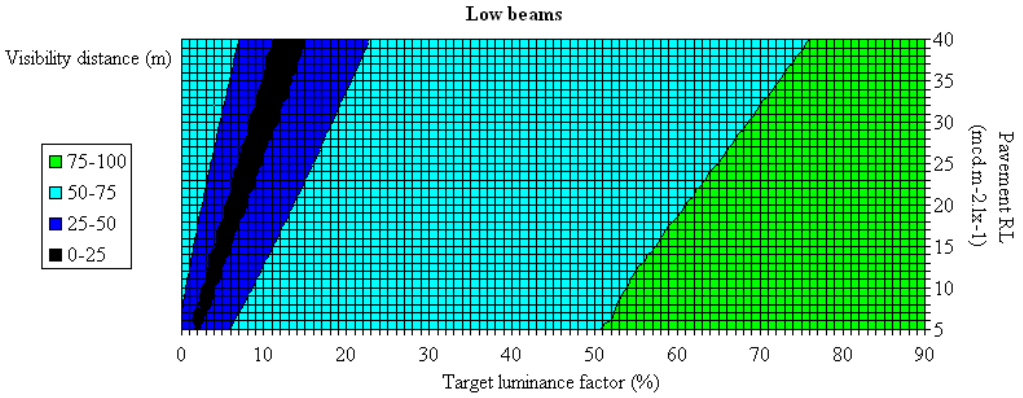

Figure D.2: Visibility distance of an 18-cm grey target in the middle of the road under low-beam illumination as a function of the target luminance factor and pavement retroreflected luminance coefficient

.

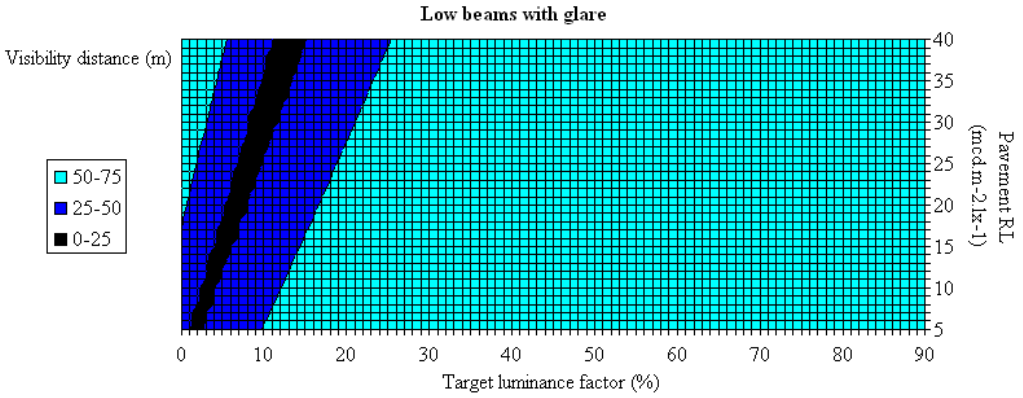

Figure D.3: Visibility distance of an 18-cm grey target in the middle of the road under low-beam illumination and with headlight glare as a function of the target luminance factor and pavement retroreflected luminance coefficient

.